3D Structure of Nanosized Catalysts by High-energy X-ray Diffraction

VALERI PETKOV

Department of Physics, Central Michigan University, Mt. Pleasant, MI 48858, USA

Currently, catalysis research is focusing on nanosized catalysts since they often show an improved activity. It is believed that the improvement is due to their greatly increased surface to volume ratio [1–3]. Evidence is mounting, however, that nanosized catalysts exhibit a good deal of structural diversity and this too may affect their activity substantially [4]. Clearly, future progress in catalysis research depends critically on the ability to obtain precise knowledge about the atomic-scale structure of nanosized catalysts. Here we show how high-energy X-ray diffraction (XRD) can accomplish this task with success.

Traditionally, the 3D structure of materials is determined by analyzing the positions and intensities of Bragg peaks in their XRD patterns. Traditional XRD studies of nanosized materials are possible but are difficult and are often imprecise. The reason is that nanosized materials show diffraction patterns with a few, if any, Bragg-like peaks and a pronounced diffuse component (see Fig. 1 below). This difficulty has pressed scientists to employ other structure-sensitive techniques such as XANES, EXAFS, TEM, and AFM. Spectroscopy techniques like XANES and EXAFS provide important information about the valence state and nearest-atomic neighbor arrangement but are not sensitive to the longer-range atomic structure in materials. Thus, for example, EXAFS would hardly discriminate between a face centered cubic (fcc) and a hexagonal close packed (hcp) type structure since both exhibit the same number of 12 first atomic neighbors. Likewise, techniques such as AFM and TEM are indispensable in revealing the material's morphology
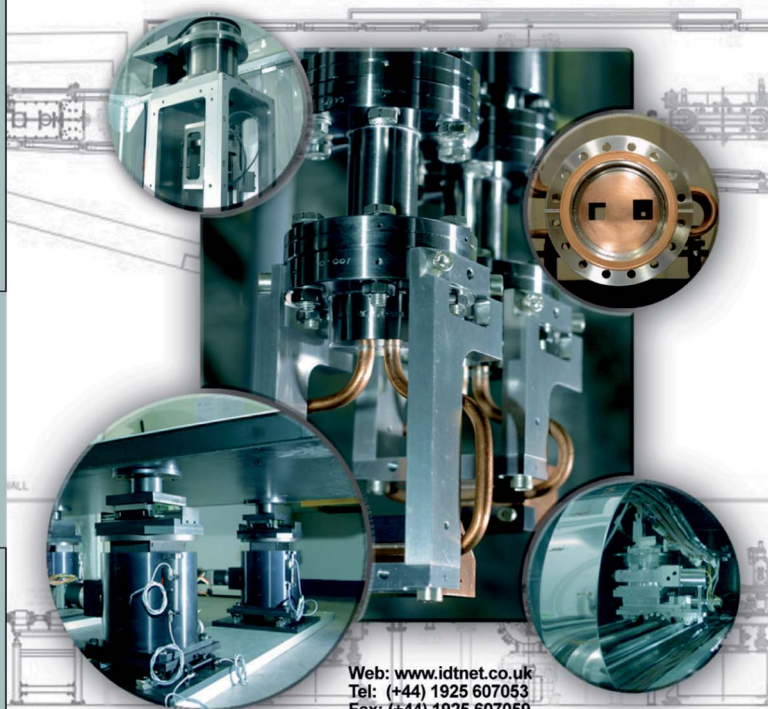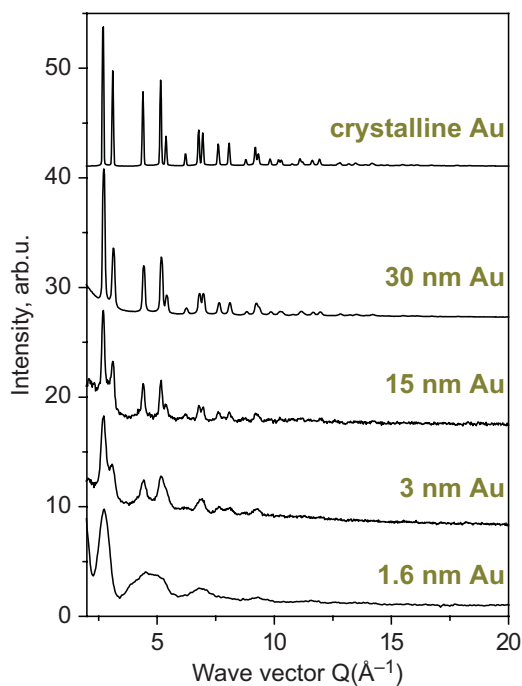
Figure 1: Experimental high-energy XRD patterns for crystalline Au and nanosized particles of Au.

but what they provide is indeed an image, i.e. a projection down an axis, and, therefore, are not very sensitive to the 3D atomic ordering inside materials either. High-energy XRD coupled to atomic Pair Distribution Function (PDF) analysis is much better suited for studying materials structured at the nanoscale [5].

High-energy XRD and atomic PDFs essentials
The frequently used reduced atomic PDF, G(r), gives the number of atoms in a spherical shell of unit thickness at a distance r from a reference atom as follows:

$$G(r) = 4\pi r[\rho(r) - \rho_o] \qquad (1)$$

where $\rho(r)$ and ρ_o are the local and average atomic number densities, respectively, and r is the radial distance. As defined, it oscillates around zero and shows positive peaks at distances separating pairs of atoms, thus reflecting the atomic ordering in materials. The PDF G(r) is the Fourier transform of the experimentally observable total structure function, S(Q), i.e.

$$G(r) = (2/\pi) \int_{Q=o}^{Q_{max}} Q[S(Q)-1]\sin(Qr)dQ, \qquad (2)$$

where Q is the magnitude of the wave vector ($Q = 4\pi\sin\theta/\lambda$), 2θ is the angle between the incoming and outgoing X-rays, and λ is the wavelength of the X-rays used [5]. X-ray diffraction usually employs the so-called

Faber-Ziman type structure function, S(Q), related to the coherent part of the diffraction pattern, $I^{coh.}(Q)$, as follows:

$$S(Q) = 1 + \left[I^{coh.}(Q) - \sum c_i \left| f_i(Q) \right|^2 \right] / \left| \sum c_i f_i(Q) \right|^2, \qquad (3)$$

where c_i and $f_i(Q)$ are the atomic concentration and X-ray scattering factor, respectively, for the atomic species of type i. As can be seen from Eqs. (1–3), the atomic PDF is simply another representation of the experimental XRD data. However, employing high-energy XRD and analyzing the experimental data in real space is advantageous, especially when studying nanosized catalysts. First, as Eq. 3 implies, the *total* scattering, including Bragg-like peaks as well as diffuse (non-Bragg-like) scattering, contributes to the PDF. In this way both the distinct atomic order, manifested in the Bragg-like peaks, and all structural "imperfections" (e.g. greatly reduced particle size, strain, defects, etc.) that are responsible for its limited extent, manifested in the intense diffuse component of the XRD pattern, are reflected in the experimental PDF for a nanosized catalyst. Second, by using high-energy X-rays high values of Q can be accessed and, hence, experimental PDFs of improved real-space resolution can be obtained [6]. And third, the atomic PDF is barely influenced by diffraction optics and experimental factors since these are accounted for in the step of extracting the coherent intensities from the raw XRD data (see Eq. 3). This makes the PDF an experimental quantity that gives directly relative positions of atoms, enabling a convenient structure search and refinement [3,7–9].
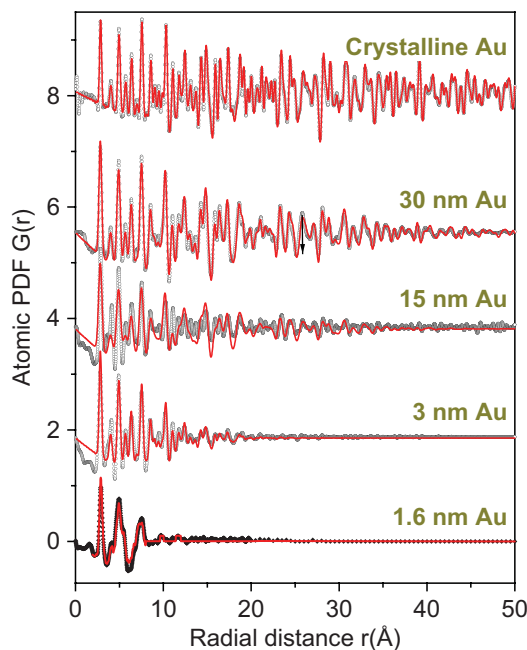
Figure 2: Experimental (symbols) atomic PDFs for crystalline Au and nanosized particles of Au. Theoretical PDFs (line in red) computed from structure models as explained in the text are shown as well.

Examples of high-energy XRD studies of nanosized catalysts

Bulk gold is exceptionally inert. Nanosized gold particles are, however, catalytically very active. The reason for the exceptional catalytic activity of Au nanoparticles is not well known but it is believed that their distinction from the bulk structure contributes to it. Experimental XRD patterns for 30, 15, 3, and 1.6 nm Au particles in aqueous solution are shown in Fig. 1. The XRD pattern for bulk Au (crystalline grains several hundreds of nm in size) is also shown. The data were obtained using high-energy XRD as explained in refs. [3, 9]. Sharp Bragg peaks are present in the XRD pattern for bulk Au, reflecting its fcc-type crystal structure. The XRD patterns for nanosized Au samples become progressively diffuse in nature with diminishing the particle size. Such diffraction patterns, in particular those for 3 nm and 1.6 nm Au particles, are difficult to analyze by traditional approaches that rely on sharp Bragg peaks. However, when considered in terms of the corresponding atomic PDFs the diffraction data lend themselves to structure analyses. Atomic PDFs extracted from the diffraction patterns of Fig. 1 are shown in Fig. 2. As can be seen in the

figure, the PDF for bulk Au exhibits a series of well-defined peaks to high real-space distances as can be expected for a perfectly crystalline material. The experimental data can be approximated very well in terms of a structure model based on an fcc-type lattice (S.G. *Fm-3m*) with a 4 atom unit cell, 4.07 Å in length [9]. The very good agreement documents the fact the atomic PDFs accurately reflect the 3D atomic structure of materials. The experimental PDFs for 30, 15, and 3 nm particles too are well reproduced by fcc-type structure models. These models, however, exhibit many structural imperfections, and the number of the imperfections increases with diminishing the particle size (see Fig.5b in ref. [9]). The experimental PDF for 1.6 nm Au particles, however, cannot be explained in terms of models featuring periodic structures, including an fcc-type lattice. On the other hand, a structurally disordered, non-periodic model (see Fig. 3c) generated by reverse Monte Carlo (RMC) simulations does a very good job in approximating all details in the experimental data as discussed in [3]. A 147-atom fragment of the fcc lattice of bulk gold, and a truncated octahedron of 140 atoms resulted from Density Functional Theory (DFT)
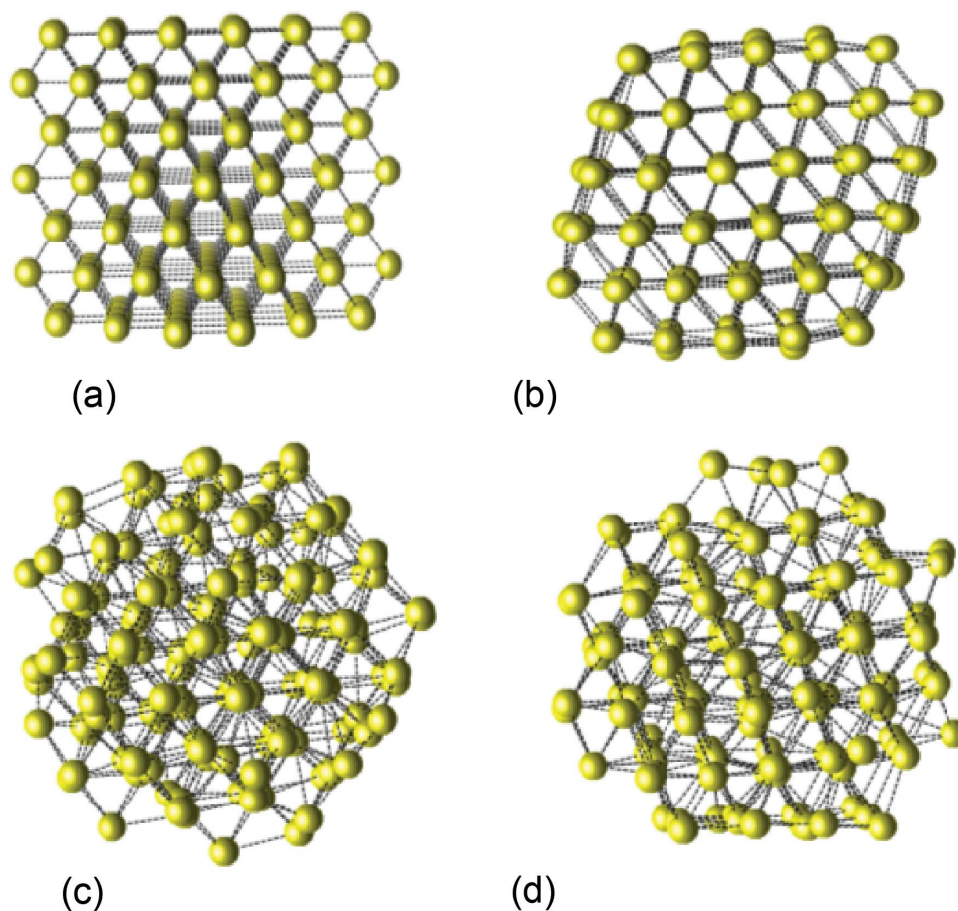
Figure 3: Fragment of the fcc lattice of bulk Au (a), 140 atom truncated octahedron as generated by DFT alone, (b) and RMC generated models of wet (c) and dry (d) 1.6 nm Au (147 atom) particles.
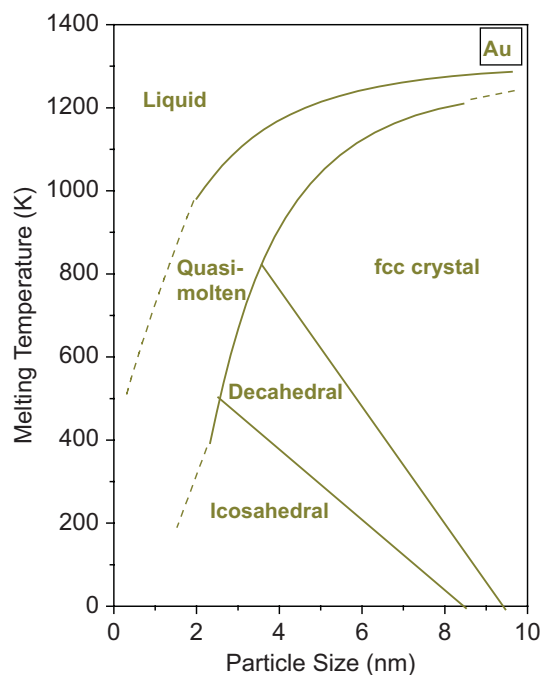
Figure 4: Theoretical phase diagram of nanosized Au [10]. Reprinted with author's permission.

model calculations alone are shown in Fig. 3a and 3b, respectively. Note that, when not refined against experimental PDF data, DFT theory predicts a model structure (i.e. a truncated octahedron) that is very well-ordered internally, periodic and, hence, with a regular shape. As can be seen in Fig. 3c the RMC constructed structure model shows signatures of local fcc-type ordering but is essentially non-periodic and, hence, not regular in shape. The lack of periodicity in the 3D structure of nanosized catalysts, such as 1.6 nm Au particles studied here, may have an important implication on their properties. In particular, the surface of such catalyst may not necessarily be made of a family of regular atomic lattice planes but become somewhat curved and/or less densely packed with atoms. Also, as recently shown [4], the electronic/band structure and, hence, the way the material's surface and adsorbates interact may be quite different for nanosized catalysts with a periodic and non-periodic 3D structure. This may render nanosized catalysts with a non-periodic 3D structure and irregular (e.g. curved) shape catalytically more (or less) active than nanosized catalysts with a periodic 3D structure and faceted shape.

Indeed, the presence of a great deal of structural diversity at the nanoscale was predicted long ago but somewhat neglected in catalysis research. A theoretical phase diagram of nanosized Au, as derived by Marks [10], is shown in Fig. 4. As theory predicts non-periodic and heavily disordered (i.e. "quasimolten"), not-periodic but locally well-ordered (e.g. icosahedral) as well as 3D periodic and well-ordered structures (e.g. fcc-type lattice) may occur in Au particles of size less than 10 nm. Note that this is exactly the range of sizes targeted for catalysis applications. Clearly, the structure

of 1.6 nm Au particles studied here is of the "quasimolten"-type occupying the left-hand side of Marks' diagram while that of 3 nm Au particles belongs to the right-hand side of that diagram. Interestingly, the structure of 1.6 nm Au particles becomes more ordered, i.e. crystal-like, when they are fast dried. This is well demonstrated by the experimental data shown in Fig. 5a. As can be seen in the figure, the peaks in the PDF for dry 1.6 nm Au particles are sharper than those in 1.6 nm Au particles in aqueous solution. A structure model obtained by an RMC fit to the PDF data for dry 1.6 nm Au particles [3] is shown in Fig. 3d. Clearly, it belongs more to the right- than to the left-hand side of Marks' diagram.

Structural phase transformations in nanosized catalysts triggered by relatively small environmental and/or temperature changes such as drying may not be a surprise since the energy difference between "quasimolten," "icosa/decahedral," and "fcc"-type structures are rather small [10]. Indeed, our studies show that the binding energy of the "quasimolten"-type structure shown in Fig. 3c is −2.82 eV/Au while that of the decahedral-type structure shown in Fig. 3b is −2.86 eV/Au [3]. For reference, the binding energy for bulk Au is −3.05 eV/Au.

It should be pointed out that not only the post-preparation treatment (e.g. drying) but the preparation conditions too may affect the atomic-scale structure, and hence, properties of nanosized catalysts. Experimental atomic PDFs for 1.7 nm Pt particles are shown in Fig. 5b. As the data show, Pt nanoparticles made with a virtually free surface [11] have much
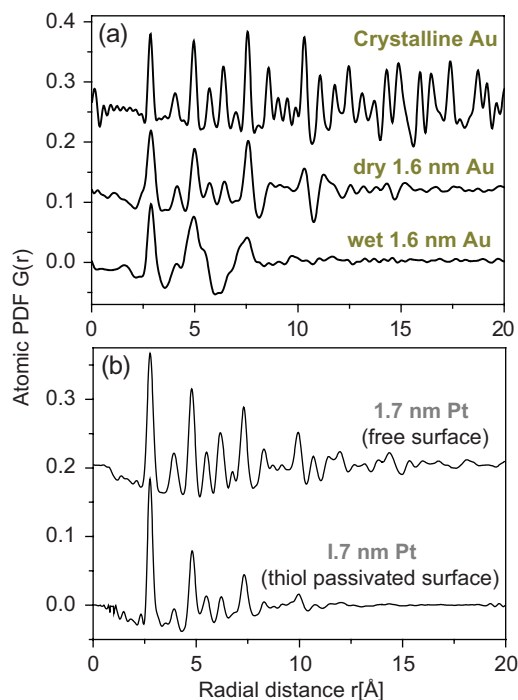
Figure 5: Experimental atomic PDFs for crystalline Au and 1.6 nm Au particles in aqueous solution (wet) and dried (a). Experimental atomic PDFs for 1.7 nm Pt particles with a free- and thiol-passivated surface (b).

more ordered, i.e. crystal-like, structure than those with a thiol-passivated surface [12]. Also, it is worth nothing that the structural diversity is a property inherent not only to nanosized catalysts smaller than 10 nm as theory predicts. Experimental studies have found that 26 nm particles of Pd, which like Au and Pt is always an fcc metal while in bulk, may also exhibit a heavily disordered, non-periodic structure [13].

Conclusion

Depending on the particular technological route, the post-preparation and/or the operating conditions (see Fig. 5), nanosized catalysts may adopt substantially different atomic-scale structures and, hence, exhibit different properties even when their composition and surface area are essentially the same. That is why the 3D structure of nanosized catalysts should be determined with due care and the properties considered in terms of the factual structure basis, be it of a "non-periodic" or "periodic" type. Thanks to their high penetration depth and the ability to access high-Q values, high-energy XRD and PDF analysis can deliver such information for nanosized catalysts with any degree of structural coherence (see Fig. 2) and in any environment (e.g. air, liquid, etc.). Also, the high flux and modern detectors make it possible to study nano-catalysts-adsorbate interactions [7], supported nanosized catalysts [14], as well as to conduct *in-situ* kinetic studies [15]. Undoubtedly catalysis research will benefit from employing high-energy XRD on a more regular basis than now, taking advantage of the rapidly increasing number of high-energy synchrotron sources worldwide.

References

1. H. Zhang, et al., *Nature* **424**, 1025–7 (2003).
2. P. Crespo, et al., *Phys. Rev. Lett*. **93**, 087204–7 (2004).
3. V. Petkov, et al., *J. Phys. Chem*. C **112**, 8907–11 (2008).
4. Y. Sun, et al., *J. Am. Chem. Soc*. **129**, 15465–7 (2007).
5. V. Petkov, *Materials Today* **11**, 28–38 (2008).
6. V. Petkov, et al., *Phys. Rev. Lett*. **83**, 4089–92 (1999).
7. N. Bedford, et al., *J. Phys. Chem*. C **111**, 18214–19 (2007).
8. V. Petkov, et al., *Phys. Rev. B* **69**, 085410–6 (2004).
9. V. Petkov, *Phys. Rev. B* **72**, 195402–7 (2005).
10. L.D. Marks, *Rep. Prog. Phys*. **57**, 603–649 (1994).
11. M. Knecht, et al., *Chem. Mat*. **20**, 5218–28 (2008).
12. C. Dablemont, et al., *Langmuir* **24**, 5832–41 (2008).
13. V. Petkov, et al., *J. Phys. Chem*. C **111**, 714–20 (2007).
14. W. Dmowski, et al., *Z. Kristallogr*. **222**, 617–24 (2007).
15. P. Chupas, et al., *J. Am. Chem. Soc*. **129**, 13822–4 (2007).

Toyama 1/2 page Hor. B& W
To be determined